

# Two-wavelength interferometry for measurement of transonic airflow in a compressor blade cascade

Pavel Psota<sup>1\*</sup>, Jan Kredba<sup>1</sup>, Marek Stašík<sup>1</sup>, Gramoz Cubreli<sup>1</sup>, Vít Lédl<sup>1</sup> and David Šimurda<sup>2</sup>

<sup>1</sup>Technical University of Liberec, Faculty of Mechatronics, Informatics and Interdisciplinary Studies, Institute of New Technologies and Applied Informatics (NTI), Studentská 2, 461 17 Liberec 1, Czech Republic

<sup>2</sup>Institute of Thermomechanics of the Czech Academy of Sciences, v. v. i., Dolejškova 1402/5, 182 00 Praha, Czech Republic

**Abstract.** This paper presents high-speed two wavelength interferometry for measuring fast phenomena, which allows to extend the dynamic range of measurement using two different wavelengths at the same time. The method was applied to measure transonic airflow through a blade cascade.

## 1 Introduction

Increasing turbine efficiency is forcing the development of new ultra-long and thin turbine blades that operate at transonic to supersonic flow rates. These long blades in the last low-pressure stages of turbines are very prone to self-excited oscillations due to flow, the so-called blade flutter, which leads to high-cycle fatigue and potentially catastrophic blade breakage. An identical problem arises in the first stages of compressors of large aircraft engines. The blade flutter is currently the most difficult design problem in terms of guaranteeing the safety and operational reliability of large turbomachines. Such phenomena must be accurately measured in order to provide necessary feedback to design more efficient turbomachines and improve the computational models used in numerical flow simulations.

Due to the presence of density gradients, the compressible fluid flow is well suitable for an investigation using optical methods which are sensitive either to the refractive index - interferometry, or to a refractive index gradient (schlieren [1], shadowgraph [2]) that are very sensitive but difficult to quantify.

Interferometry is one of the basic tools in the field of flow visualization. Digital interferometric methods using sensitive high-speed cameras [3] make it possible to quantify the quantities of airflow fields with high accuracy and spatial resolution. Interferometric techniques are based on "encoding" the optical phase of a wave to a measurable intensity in the form of interference fringes. In the case of steep or step changes in the measured quantity, the interference structure may be undersampled and thus information may be lost. Examples may be shock waves that show a step change in air density. For the measurement of phenomena with high gradients, where the undersampling of the fringe pattern occurs, it is possible to use two wavelength interferometry. This paper presents interferometric technique for research of compressible fluid flow in a

wind tunnel facility [4]. The technique has been developed in order to enhance understanding of the blade flutter phenomenon in turbomachines, in particular for transonic flow conditions. The developed technique is sensitive and accurate yet easy to use under conditions typical for aerodynamic labs.

## 2 Dynamic two-wavelength interferometry

Digital interferometry is an accurate and full-field measurement method that is sensitive to the change in the phase of an optical wave. Superposition of two coherent waves generates an interference pattern. Introducing a tilt between reference and object arms in interferometer results in SCI. Assuming the tilt in x-direction only, the captured interference pattern on a CCD or CMOS camera sensor can be expressed as

$$I(x, y) = A(x, y) + B(x, y) \cos(\varphi(x, y) + 2\pi f_0 x), \quad (1)$$

where  $f_0$  denotes spatial carrier frequency due to the tilted wave, A stands for additional term and B is the signal modulation.

Such interference pattern is further Fourier transformed and spatially filtered to select the portion of the signal around the spatial frequency  $f_0$ . Bandwidth of the band-pass filter influences the lateral resolution of measurements. An inverse Fourier transform results in complex field  $C_F$  and hence the interference phase can be calculated as:

$$\varphi(x, y) = \arctan\left(\frac{\text{Im}(C_F(x, y))}{\text{Re}(C_F(x, y))}\right). \quad (2)$$

Let us assume a phase measurement at steady/reference state without presence of fluid flow

---

\* Corresponding author: [pavel.psota@tul.cz](mailto:pavel.psota@tul.cz)

resulting in the complex field  $C_{F0}$ . Such measurement carries information about interferometer optical aberrations including aberrations introduced by e.g. optical windows of the wind tunnel experiment. Other measurements performed with the presence of a phenomenon ( $C_{F1}$ ) can be related to the reference state by the interference phase:

$$\Delta\varphi(x, y) = \arctan\left(\frac{\text{Im}(C_{F1}(x, y)C_{F0}^*(x, y))}{\text{Re}(C_{F1}(x, y)C_{F0}^*(x, y))}\right) \quad (3)$$

in order to suppress undesired optical aberration. The interference phase can be used to determine the desired physical quantity such as temperature [5], shape [6], refractive index [7], vibration amplitudes [8] or density/isentropic Mach number as in this particular case.

So far, we have considered only single wavelength SCI, with the unambiguity range of the wavelength of the light. Due to Nyquist criteria, the real range of unambiguity is limited to a half-wavelength. However, for the measurement of phenomena with large gradients, it is necessary to extend the unambiguity interval. This can be achieved by two-wavelength interferometry. For dynamic measurements two-wavelength SCI is applied. Two-wavelength interferometer interferometry can be realized by adding a second coherent source of wavelength  $\lambda_2$  to the previously described technique with  $\lambda_1$ . Let us now assume SCI interferometer with two independent laser sources with wavelengths  $\lambda_1, \lambda_2$ .

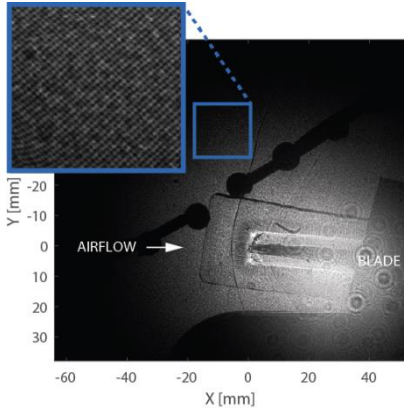


**Fig. 1.** Multiplexed interferogram captured by a camera.

Both object waves with  $\lambda_1, \lambda_2$  follow the same path through the testing section while both reference waves with  $\lambda_1, \lambda_2$  propagates independently and can be separately adjusted. In one camera shot, a multiplexed interference pattern  $I$  of two independent overlapping interference patterns  $I_{\lambda_1}, I_{\lambda_2}$  is captured, see Fig. 1.

If the spatial carrier frequencies for both wavelengths are set properly (by adjusting angles of reference beams), information from both wavelengths can be separated in the Fourier domain during the filtering, see Fig. 2a.

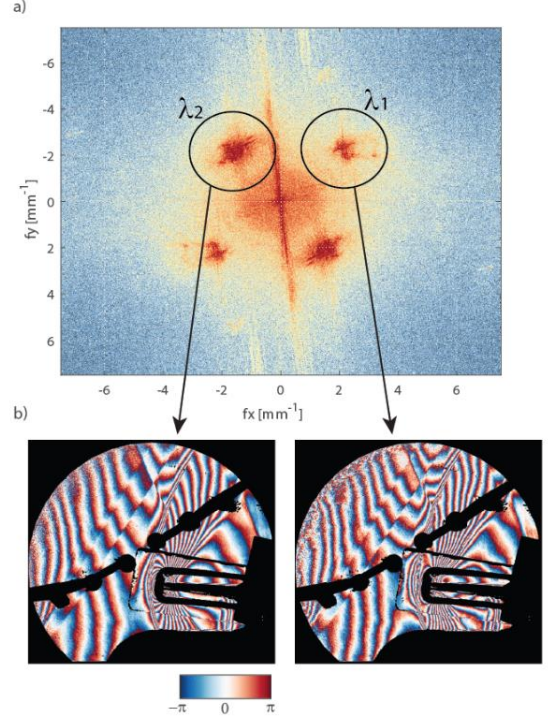


**Fig. 2.** a) magnitude in logarithmic scale of the Fourier transform of the interferogram with the denoted terms corresponding to both wavelength. The circles mark bandwidth of the filter and retrieved phases for both wavelengths are shown in b).

The filtering is carried out around the two carrier frequencies with different wavelength resulting in two interference phase maps  $\Delta\varphi_{\lambda_1}(x, y)$  and  $\Delta\varphi_{\lambda_2}(x, y)$ , see Fig. 2b. In order to extend the unambiguity range, a beat fringe pattern further referred as synthetic phase map is generated:

$$\phi(x, y) = \Delta\varphi_{\lambda_2}(x, y) - \Delta\varphi_{\lambda_1}(x, y). \quad (4)$$

Values in (4) are naturally constrained by  $-\pi < \phi \leq \pi$ . However, the synthetic wavelength is much larger than individual wavelengths  $\lambda_1, \lambda_2$  and so the unambiguity range, with the synthetic wavelength defined as:

$$\Lambda = \frac{\lambda_1\lambda_2}{\lambda_2 - \lambda_1}. \quad (5)$$

From (5) follows that the unambiguity range can be adjusted by set of proper wavelengths. On the other hand, the uncertainty of interferometric measurements is proportional to the wavelength and thus the synthetic phase  $\phi$  with  $\Lambda$  suffers from more noise than the individual phase fields  $\Delta\varphi_{\lambda_1}$  and  $\Delta\varphi_{\lambda_2}$ . It is therefore advantageous to combine both large unambiguity range of  $\phi$  and low uncertainty of  $\Delta\varphi_{\lambda_1}$  or  $\Delta\varphi_{\lambda_2}$ . As a result unwrapped interference phase  $\Delta\varphi$  free of  $2\pi$  jumps due to harmonic nature of light waves is retrieved, see Fig. 3.

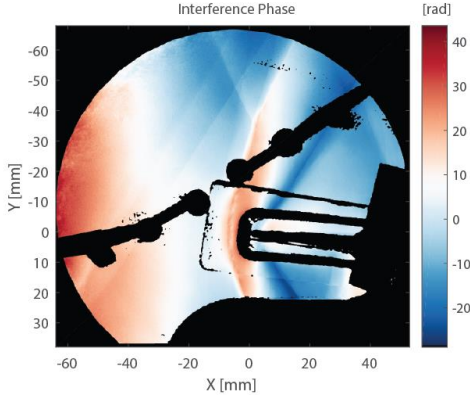


Fig. 3. Unwrapped interference phase.

### 3 Experimental arrangement

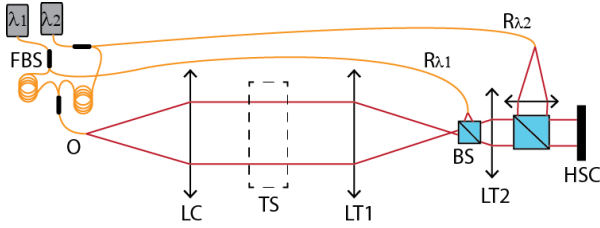


Fig. 4. Experimental arrangement:  $\lambda_1$ ,  $\lambda_2$ - lasers; FBS-fiber beam splitters; O-object wave;  $R_{\lambda_1}$ ,  $R_{\lambda_2}$ -reference waves; LC- collimating imaging lens; TS- testing section; LT1,LT2- lenses; BS-beam splitter; HSC- high-speed camera.

The experimental arrangement was built as a fiber based Mach-Zehnder interferometer, see Fig. 4. Laser beams were generated by single-mode diode laser Toptica DLC pro with wavelength  $\lambda_1=632\text{nm}$  and a pigtailed single-frequency distributed feedback laser of the wavelength  $\lambda_2=773\text{nm}$ . The laser beams were split using fibersplitters (FBS) into the reference wave ( $R_{\lambda_1}$ ,  $R_{\lambda_2}$ ) and another FBS was used to combine both wavelengths into the object wave (O). The reference waves were guided by optical fibers to the non-polarizing beamsplitters (NBS), while the free-space object wave passed through a collimating imaging lens LC, which sent light through the test section of a testing section (TS), before passing through a lens LT1. Lenses LT1 and LT2 acted as beam expander with magnification of  $\text{Mag}\approx 0.18$  as well as an imaging system focusing in the middle of TS. Both reference and object waves were recombined by the beamsplitter (NBS) and collimated by LT2. The object wave impinged normally the digital camera sensor (HSC) - Phototron FASTCAM Mini WX100 high-speed camera having resolution of  $2048\times 2048$  pixels ( $10\mu\text{m}\times 10\mu\text{m}$  pixel size) with a frame rate of 1080fps in order to avoid blurring. The reference waves were tilted with angles in order to introduce the required spatial carrier frequencies.

### 4 Measurement results

A planar compressor blade cascade with five blades was mounted in the test section of a transonic wind tunnel (see Fig. 5). The blades have a chord length of 120 mm, span  $L=160$  mm (i.e. aspect ratio of 1.33) and maximum

thickness 5.94 mm. The cascade stagger angle is  $41.5^\circ$ . During measurements, the flow velocity is monitored using Prandtl probe at the inlet of the test section and two rows of static pressure taps on the test section sidewall upstream and downstream of the blade cascade. Inlet Mach number of the airflow was set to be  $M_{in}=1$ .

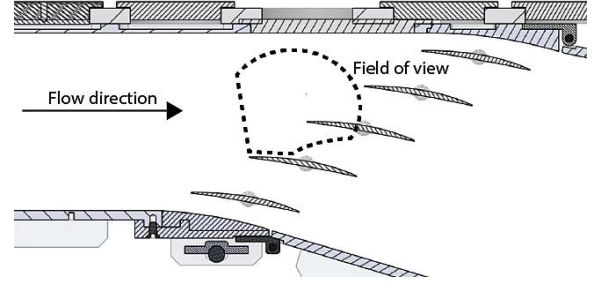


Fig. 5. The blade cascade with interferometer's field of view

The test section is mounted in a suction-type high-speed modular wind tunnel of the Institute of Thermomechanics of the Czech Academy of Sciences, see Fig. 6.

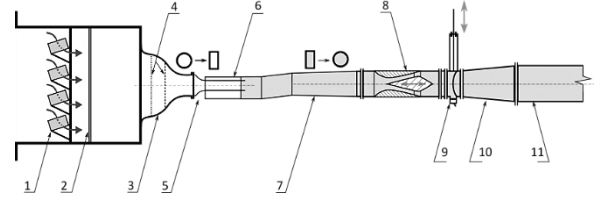


Fig. 6. Schematic of the wind tunnel: 1 - silica-gel dryer, 2 - pebble and cloth filter, 3 - circular contraction, 4 - honeycomb and screen, 5 - contraction and cross section change insert, 6 - test section, 7 - diffuser and cross section change insert, 8 - control nozzle, 9 - quick acting valve, 10 - diffuser, 11 - pipe connection to vacuum chamber.

The wind tunnel consists of a free atmospheric entry, dryers and filters, contraction leading to the test section and exit parts with control and safety valves connected to a high-volume vacuum chamber.

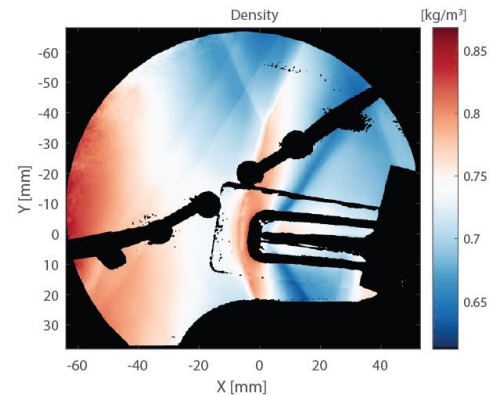


Fig. 7. Density distribution

The measured multiplexed interference pattern is processed in order to retrieve the unwrapped interference phase  $\Delta\varphi$  by two-wavelength technique. The interference phase is then linked to density (see Fig. 7) using

$$\rho(x, y) = \rho_{ref}(x_0, y_0) + \frac{\Delta\varphi(x, y)\lambda}{2\pi LK} \quad (6)$$

In (6),  $L$  denotes the wind tunnel testing section width,  $K$  is the Gladstone-Dale constant and  $\rho_{ref}$  is the reference density calculated from a static pressure sensor located in the position  $(x_0, y_0)$ .

For the case of isentropic compressible flow of ideal gas, the measured density  $\rho(x, y)$  can be further linked with the isentropic Mach number (see Fig. 8) by the following equation:

$$M_i(x, y) = \sqrt{\frac{2}{\kappa - 1} \cdot \left( \left( \frac{\rho_{in}}{\rho(x, y)} \right)^{\kappa - 1} - 1 \right)} \quad (7)$$

where  $\rho_{in}$  is the inlet air density and  $\kappa=1.4$  denotes the heat capacity ratio for an ideal diatomic gas.

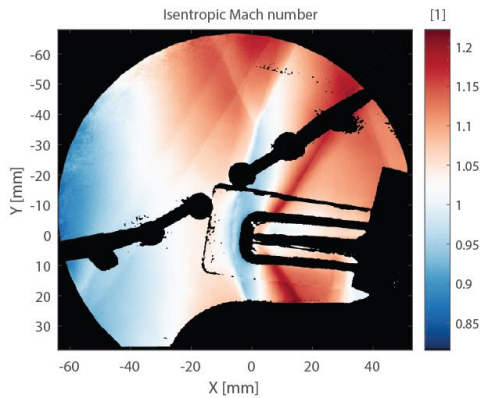


**Fig. 8.** Isentropic Mach number

The spatial resolution  $150 \mu\text{m}$  is in our particular case determined by the bandwidth of the applied band-pass filter. Shocks can be enhanced by plotting the Mach number distribution gradient in the  $x$  direction, see Fig. 9

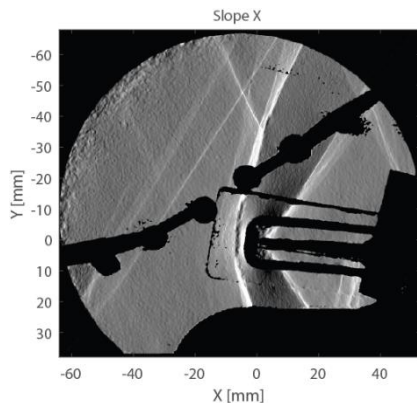


**Fig. 9.** Slope of the isentropic Mach number distribution in  $x$ -direction

## 5 Conclusion

This paper presents a very effective technique for investigating compressible fluid flow with high gradients. The developed two-wavelength interferometric technique with extended range of unambiguity is very sensitive and accurate yet easy to use even under pretty harsh environmental conditions (vibrations, flow instability, etc.) typical for aerodynamic labs.

The interferometer employs a high-speed camera, fiber optics and available “off-the-shelf” optics and

optomechanics. The interferometer consists of an illumination unit with two laser sources and a sensing unit, each weighing less than 5kg. An optical fibers deliver reference waves from the illumination to the sensing unit while the object wave carrying both wavelengths propagates through a measured volume into the sensing unit. Reference and object waves are superposed and a multiplexed interference pattern is captured by the high-speed camera. The construction of the interferometer together with the fiber optics ensure high compactness and portability of the system.

Moreover, a single-shot quantitative data processing based on introducing a spatial carrier frequency and processing in Fourier domain allows for almost real-time quantitative processing suitable also for very fast evolving phenomena. The two-wavelength technique enables the measurement of high gradients while maintaining the interferometric accuracy of one wavelength.

The interferometer has been successfully applied to measure airflow through a blade cascade and results are used to better understand the blade flutter.

## Acknowledgements

This research was supported by the Grant Program of the Technical University of Liberec (project number PURE-2020-3010).

## References

1. M. Passmann, S., F. Joos, *Int. J. Turbomach. Propuls. Power*, **5**, 1 (2020)
2. M. Hijikuro, M. Anyoji, M. Hijikuro, M. Anyoji, *J. flow control meas. visual.*, **8**, 4 (2020)
3. H. Tang, P. Razavi, K. Pooladvand, P. Psota, N. Maftoon, J. J. Rosowski, C. Furlong, J. T. Cheng, *Appl. Sci.*, **9**, 14 (2019)
4. P. Psota G. Cubreli, J. Hala, D. Simurda, P. Sidlof, J. Kredba, M. Stasik, V. Ledl, M. Jiranek, M. Luxa, J. Lepicovsky, *Sens.*, **21**, 23 (2021)
5. P. Psota, P. Dancova, G. Cubreli, V. Ledl, T. Vit, R. Dolecek, O. Matousek, *Int. J. Therm. Sci.*, **145** (2019)
6. P. Psota, H. M. Tang, K. Pooladvand, C. Furlong, J. J. Rosowski, J. T. Cheng, V. Ledl, *Opt. Express*, **28**, 17 (2020)
7. P. Mokry, P. Psota, K. Steiger, J. Vaclavik, R. Dolecek, D. Vapenka, V. Ledl, *J. Phys. D*, **49**, 25 (2016)
8. P. Psota, P. Mokry, V. Ledl, M. Stasik, O. Matousek, J. Kredba, *Opt Lasers Eng*, **121** (2019)